

# Design and Numerical Study of Origami-Inspired Structures for Axial Compression and Energy Absorption in Crashworthiness Applications

## Abstract

Recently origami inspired structures have become of great interest because of their potential to provide lightweight, deployable, energy-absorbing structures for impact mitigation in the automotive and aerospace industries. This study illustrates a numeric computational framework utilizing Rhino with Grasshopper for parametric origami CAD modeling, and Ansys Workbench to perform finite element analysis of origami structures in axial compression. Origami patterns, including Miura-ori and Kresling patterns, were modeled and tested using axial compression to characterize load bearing capabilities, deformation mechanisms, and energy absorption efficiencies. Simulation results show that both Miura-ori and Kresling patterns are able to resist peak loads and dissipate energy more effectively than structures of greater simplicity due to their stable concertina deformation modes. The study suggests that origami geometries can be calibrated to improve crashworthiness performance and demonstrates their applicability for lightweight crashworthy components. This study contributes significant insight for the optimization and future fabrication of origami-based energy absorbers for use in impact zones.

**Keywords:** Origami Structures, Miura-ori, Folded TPU, Flat TPU, Stress, Deformation, Flexibility, Stiffness, Energy absorption, ANSYS simulation.

## 1. Introduction

A variety of origami-based engineering systems have been discussed or studied because they can provide high strength-to-weight ratio, have foldability, and are energy absorbers for applications in automotive crash safety and aerospace structures. These systems use geometric design principles that are found in origami of the past to develop novel, lightweight, and collapsible components that have an inherent ability to be resilient when compressed axially. Origami designs, specifically the Miura-ori and Kresling, have again been noted for their unique mechanical properties and their ability to be incorporated into systems designed for impact mitigation or crashworthiness. This project will assess the mechanical properties of a few different origami geometries under an axial compression load through experimentation. Focus will be placed on the load-displacement response, deformations modes, and energy absorption performance of the various geometries. The research will lead to the design of next generation crashworthy structures that have low density with high performance energy absorption capacity.

## 2. Literature Review

There are numerous studies outlined in volume suggesting the mechanical versatility that can be achieved with origami based geometries. Jiayao Ma et al. [1] have proposed structures with graded stiffness based on the origami allow assuring that origami enables a tailorabile stiffness response, along the axis of compression. Xiang, Lu, and You [2] provided evidence of the substantial energy absorption that several origami inspired materials provided when compared to traditional materials when subjected to axial and impact loading. The performance of Kresling origami structures physical principles where Moshtaghzadeh and Mardanpour reported that multi-story origami formats can dissipate energy and provide scalable crash protection. Continuing the work, Leanza et al. reported functional origami utilizing smart materials to achieve adaptive deployment and response [3].

Gattas and You [4] parameterized curved-crease origami geometries, allowing for exact precision to fold and deform. Liu et al. [5] connected the areas of materials science and origami by demonstrating how the material properties and folding patterns play critical roles in the overall stiffness and mechanical response of the origami structure. Origami engineering has also been collaborating with the biomedical field, as highlighted in Johnson et al.'s review, and with programmable and shape-changing materials via active materials [6].

Comprehensive overviews by Fonseca et al. and Mou et al. discussed how pattern geometry, scaling, and material selection affect global deformation and energy absorption in origami systems [7,8]. Miura-ori, Kresling, and Miura-derivative folded patterns have been dosed as mechanical metamaterials and performance for energy absorption [9,10].

Chen et al. and Zhou et al. [11,12] have compared the design of the geometric and kinematic mechanisms through which such foldable patterns have been used for effective engineering performance. Foundational work of Lu and Yu and more recently by Song et al. and Ma and You makes it clear that a few origami pre-folds can greatly enhance the energy dissipation profile of thin-walled and square tube structures under axial crushing type loading [13,14,15].

Collectively, these works provide significant evidence supporting origami-based systems for energy absorption, protection, and recognition of fabrication and scale-up as continuing obstacles to our real-world use of these systems.

## 3. Methodology

The research approach used in this research can be generalized into two key stages: 1. Computation design of origami-inspired structures, and 2. Numerical evaluation of the crashworthiness and energy absorption characteristics of the origami-inspired structures.

### 3.1. Computational Origami Design with Rhino + Grasshopper

In order to create accurate and parametric models of the origami patterns selected, Rhino 3D software was used together with the Grasshopper visual programming plug-in. The origami geometries for the Miura-ori were modeled by defining the fold lines (mountain and valley folds) as curves and manipulating the mesh geometry within Grasshopper. Using custom scripts and available plug-ins (Crane

to run simulation of folding kinematics) allowed for accurate construction, modification, and visualization capabilities into the design capabilities of foldable structures figure1.

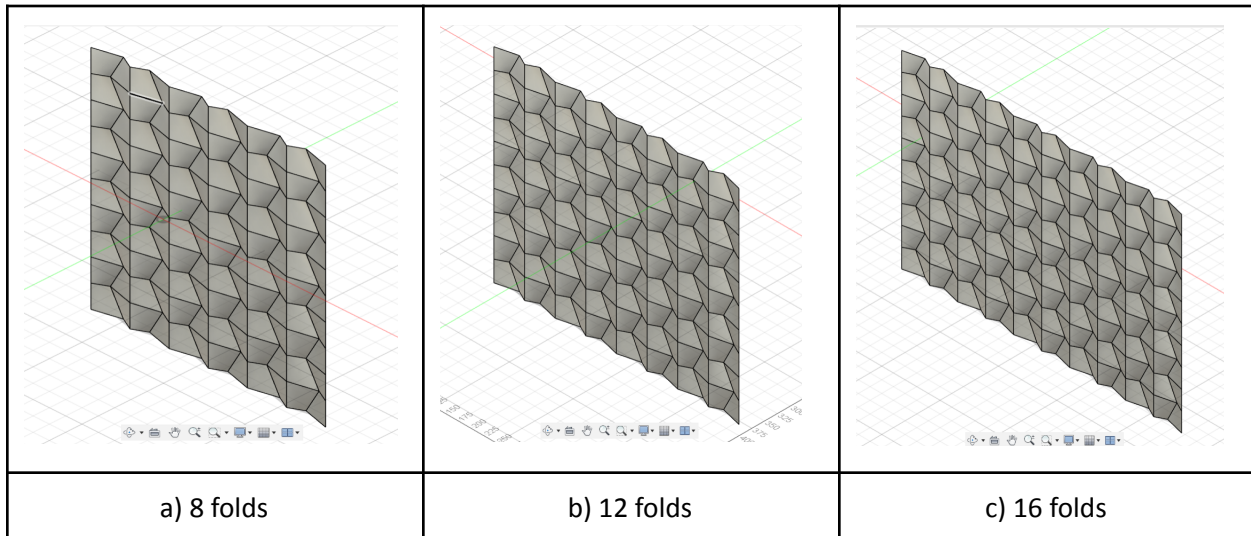


Fig 1. Origami CAD

### 3.2. Finite Element Analysis Using Ansys Workbench

The digital models which had been created in Rhino + Grasshopper were transferred from an appropriate format (e.g., STEP or IGES) and transferred to Ansys Workbench for simulation. In Ansys, the origami geometries were each meshed appropriate to thin-walled structures, thus creating an accurate representation of fold lines, and facets. The axial compression tests were simulated by applying boundary conditions and displacement-controlled loading to the models, where material properties were assigned based on actual test materials (e.g., small sheets of thin aluminum or TPU). The results were then analyzed flexibly to extract metrics such as peak load, deformation patterns, energy absorbed during compression. Ultimately, the analysis provided a systematic way to quantitatively compare different origami geometries to determine performance, such as suitability for impact reduction, based on load-bearing and energy absorption performance.

#### Miura-ori 8X9 folds:

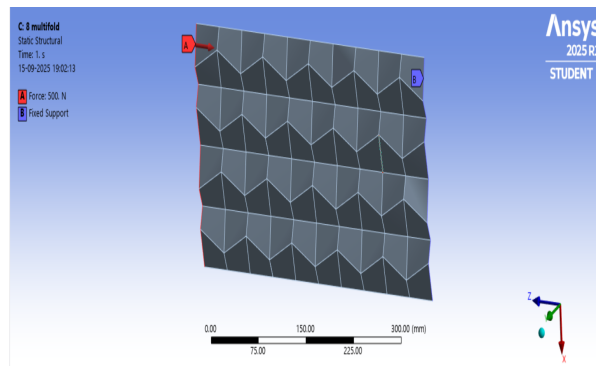


Fig 2: Force Applied and fixed support for 8X9 fold miura origami

As can be seen in Figure 2. ANSYS simulated a static structural analysis of a multilayer origami-inspired structure under an axial compression scenario. The geometry had a Miura-ori like fold pattern, and was prompted to observe the deformation characteristics along with the energy absorption. A 500 N compressive load was applied on the left-hand edge of the structure, where the right-hand edge was fixed, to simulate a uniaxial loading. The purpose of this analysis is to examine total deformation, displacement in the direction of load, equivalent stress and strain. The analysis setup permits observing the origami, the folded geometry, compressing under load, with a region of maximum stress and deformation. Gaining results from this analysis is useful to compare origami-based structural behavior with flat plates, providing an indication for the compliance and energy absorption under axial load conditions.

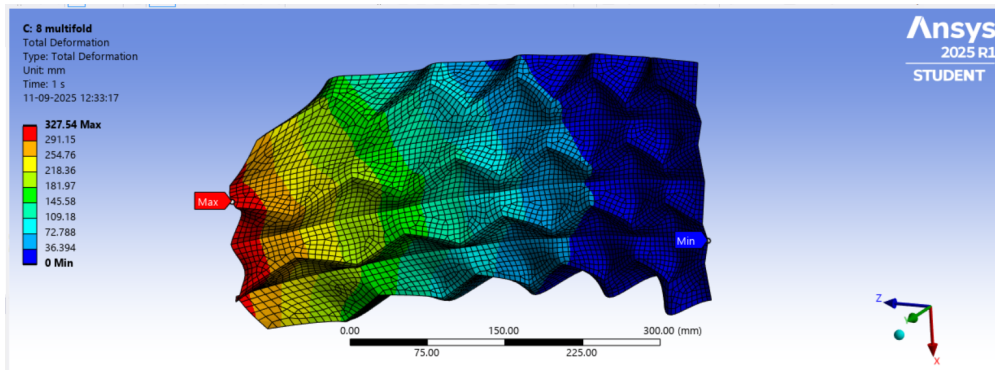


Fig 3: Total deformation for 8X9 fold origami

Figure 3. is the total deformation result of an origami structure with multiple folds subjected to a 500 N compressive load using ANSYS 2025 R1 software. The colored contour plot indicates this structures deformation in axial loading mode. The red regions adjacent to the loaded edge indicates the maximum deformation of 327.54 mm, while the blue regions at the fixed edge reflect zero displacement developed, due to the supported applied boundary condition. The colors indicate gradual transitions from blue to red to indicate how deformation is distributed through the folds and the actual regions where displacement is moderately transferred or developed in the intermediate regions (green, yellow). This final result indicates the high degree of compliance in the origami design and demonstrates plausible deformation in the structure under loading and that the energy is transferred through to the folded geometry. The observed deformation behavior suggests that multifold origami structures may be suitable for specific applications that value high crashworthiness and product the dissipation of impact energy.

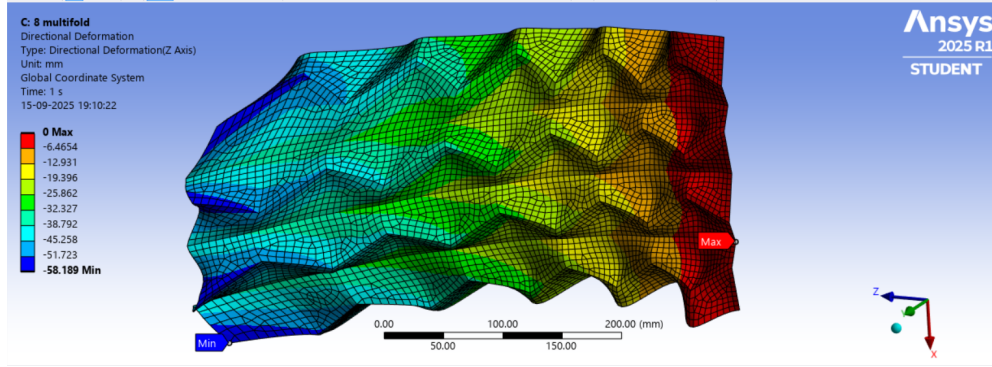


Fig 4: Directional deformation for 8X9 miura origami

Figure 4. shows the directional (Z-axis) deformation behavior of the multifold origami structure, as experienced within a 500 N compressive load. For this surface plot, the emphasis is on the displacement along the loading direction. The plotted contours show a nice color gradient from blue, as experienced at the fixed edge with little to no or negative displacement, to red for the loaded edge, highlighting an area of maximum axial deformation at 58.159 mm. The gradient maps how the externally applied force is absorbed and distributed through the folds. Notice the localized area in which the compression is greatest, concentrated close to the force applied, but also the continued stable structure at the fixed support of the origami specimen. This shows how advantageous the origami design becomes in achieving deformation in the desired direction. Consequently, the structural property of controlled folding structures can allow for high energy absorption. This is particularly advantageous in crashworthiness and impact mitigation applications where energy must be absorbed safely, but in predictable, relatively large axial displacements.

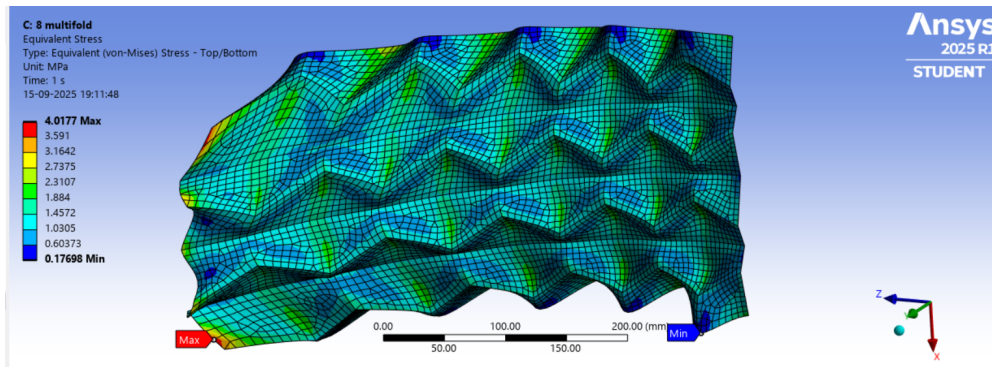


Fig 5: Equivalent stress for 8X9 miura origami

Figure 5. shows the equivalent (von Mises) stress distributions for the multifold origami structure under the 500 N compressive load, developed in ANSYS 2025 R1. The contour plot demonstrates stress distribution characteristics within the folded geometry, with the maximum von Mises stress measuring 4.0177 MPa, positioned neighbouring the loaded edge that is under the action of the applied compressive force. The blue areas demonstrate where the minimum stress (0.17668 MPa) is located, which is primarily away from the load path and towards the minimum displacement restraints of the fixed-support location. The blue presentation was cautioned as it shows where the deformation is very

limited. The areas of green/yellow present areas of reasonable stress, which supports the argument that origami folds allow the resulting loads (reactions) to be spread across multiple facets of deformation rather than confined in one area when loaded. The evidence of the stress distribution demonstrates the capacity of the multi-fold structure to allow substantial deformation, whereby the applied load can be distributed between facets within the multi-fold structure and reduce localised failure while strengthening the stability of the structure under axial compression. The folds will inherently distribute the load with the originating structure being origami-inspired; indicating it is an ideal geometry for energy absorption and crashworthiness applications, where strength and some controlled deformation is essential.

#### Miura 11X9 folds:

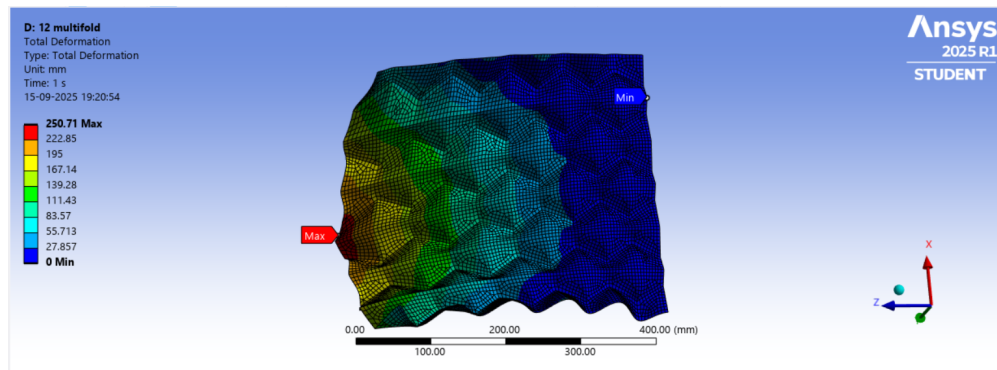


Fig 6: Total deformation for 11X9 fold origami

Figure 6. illustrates the results of total deformation for the 12-fold origami structure in (ANSYS 2025 R1) with a load of 500 N of compressive stress. The contour plot illustrates the original structure in deformation characteristics against the specified load. Deformations range between the minimum of 0 mm (blue area), and 252.71 mm (red area) as the maximum deformations for the 12-fold origami structure. The level of deformation increases when viewed along the boundary with the load at the end of the origami configuration, i.e., where the compressive load is intended, and decreases when looking at the edge of the support. The edge of the support is fixed and assumed to be fully constrained during the modeling of the process - required to remain fully constrained. This distribution indicates that the origami structure has been significantly deformed which illustrates the features of the origami structure system as a feature that can flex, dissipate and absorb energy during compression rather than remaining stiff. This is significant because it is about structural compliance. This is an intriguing aspect for engineers to understand whether any structural compliance by flexing of the origami structure deformation is of benefit in the application for energy absorption, cushioning, or impact/crash protection systems.

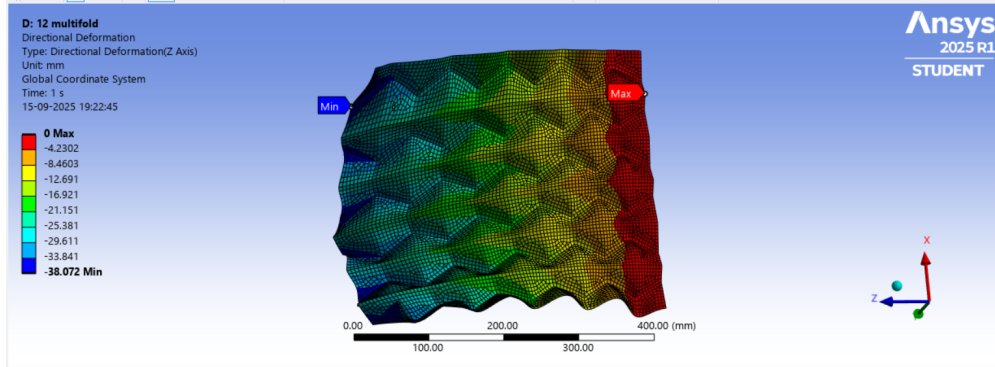


Fig 7: Directional deformation for 11X9 miura origami

Figure 7. shows the orientation dependent deformation along the Z-axis of an  $11 \times 9$  Miura origami configuration under a 500 N static compressive force, run in ANSYS 2025 R1. The color contour shows the deformation of the structure in the out-of-plane direction, showing minimum deformation at -38.072 mm (blue regions) and deformation at or near zero (red regions). The blue regions depict the area through which the structure moves downward the most, thereby indicating compression, while the red regions appear to be undisturbed. The heat maps developed from red to blue indicate the progressive deformation over the surface of the structure, and illustrate how the Miura fold is accommodating external loading by distributing strain through its folding configuration to the external load. The behavior of the structure indicates an effective capability of being able to take and accept load efficiently and controlling deformational displacement, which is highly desirable in applications such as deployable structures, impact energy absorbing mechanisms, and lightweight mechanical components.

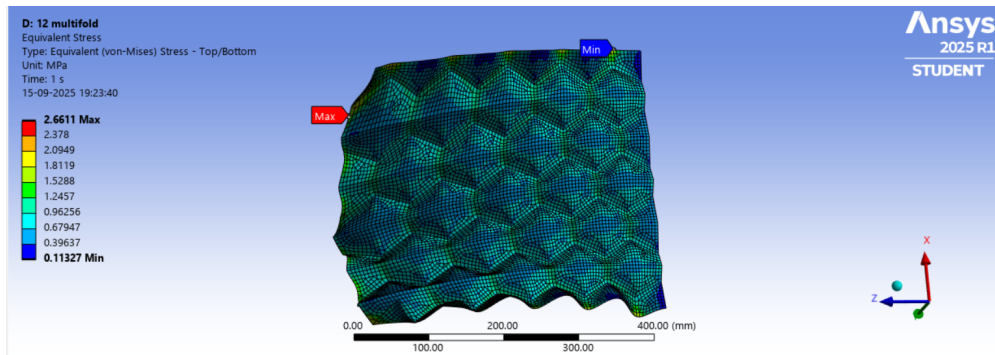


Fig 8: Equivalent stress for 11X9 miura origami

Figure 8. shows the equivalent (von Mises) stress distribution for the  $11 \times 9$  Miura origami structure when a compressive load of 500 N is applied, analysed using ANSYS 2025 R1. The contour plot illustrates how the stress is distributed throughout the structure, with values ranging from a low of 0.113 MPa (darker blue areas) to a high of 2.661 MPa (red coloured areas). The highest values of stress are near the edges and where the folds intersect, as the load transfers and geometry creates a peak in stress. Most of the surface is positioned in the green and light blue colours, showing that the Miura origami pattern does a good job of spreading the load throughout the structure and this reduces the potential for material failure while the structure is under moderate loading conditions. This representation is indicative of the

structural efficiency of Miura origami, allowing deformation of the material without exceeding low levels of stress throughout most of the structure.

### Miura 15X9 folds:

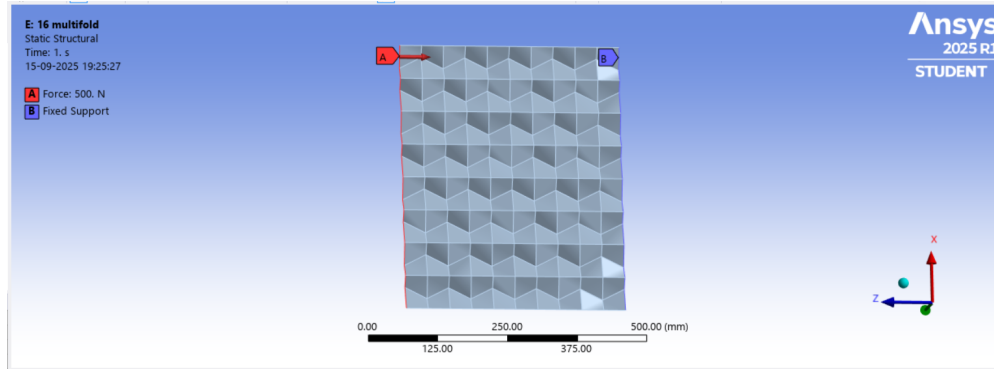


Fig 9: Force Applied and fixed support for 15X9 fold miura origami

Figure 9. depicts both the loading and boundary conditions for the Miura origami structure, 15×9-fold, in ANSYS 2025 R1. A static structural analysis is done with a compressive force of 500 N acting on the left vertical edge (shown in red), while the right vertical edge is fixed (shown in blue) to prevent all degrees of freedom. This boundary condition simulates uniaxial compression and allows the origami structure to deform under the load while scarring a stable base on one side. The simulation environment is set to 22 °C enabling standard material behavior. This configuration also makes it possible to evaluate deformation, stress distribution, and energy absorption performance of the origami structure under real loading conditions.

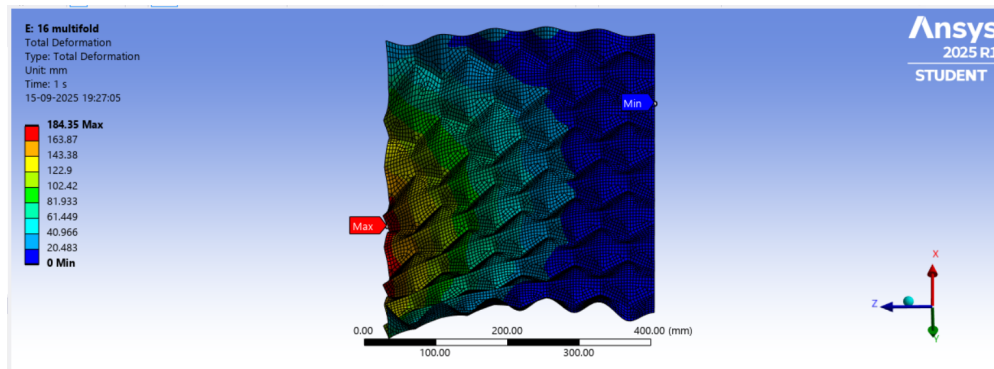


Fig 10: Total deformation for 15X9 fold origami

Figure 10. demonstrates the results of total deformation for the 15x9 fold Miura origami structure, which was tested under a compressive loading of 500N on the left edge. The deformation contour plot visually represents the displacement across the entire structure; the maximum deformation is 184.35 mm (illustrated in red), occurring approximately at the location of applied load and the minimum deformation, nearly 0 mm (illustrated in blue), located near the fixed support. The gradual transition from red to blue is indicative of a smooth deformation mechanism where the origami structure is able to absorb and redistribute the applied load. This finding is important for understanding a fold's behavior with respect to flexibility and energy absorption (e.g., like how it buckles), and whether or not the structure could tolerate a compressive load without failure.

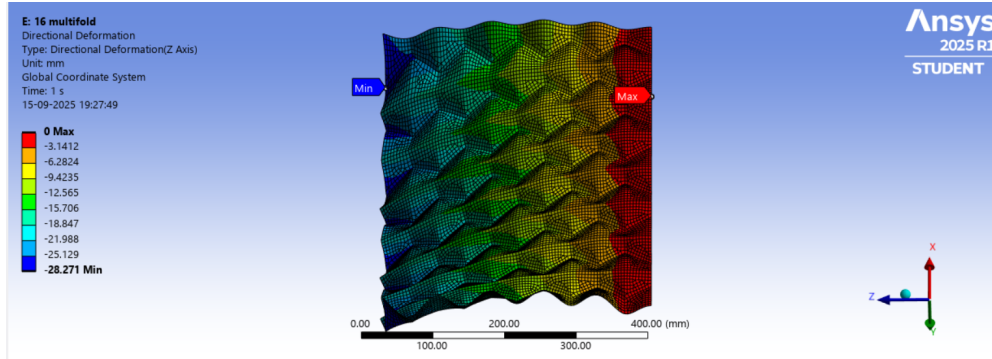


Fig 11: Directional deformation for 15X9 miura origami

Figure 11. depicts a simulated result from ANSYS 2025 R1 Student Edition, which shows the directional deformation analysis of a 15x9 Miura Origami structure. The model is being tested in the Z-axis direction under structural deformation conditions. The color contour plot exhibits the magnitude of deformation that occurs throughout the origami panel, with a color scheme illustrating the value of deformation. The maximum deformation shows to be about 6.1426 mm (shown in red, on the edge of the structure to the right), and the minimum is about -28.271 mm (shown in blue, on the left edge). This outcome indicates a significant out-of-plane, or directional, bending behavior and is consistent for Miura-patterned structures under loads exerted mechanically. The simulation shows fixed supports, as well as the applied loads in the outline tree to the left, and the results show time step 1, the response (deformation) at this particular time step. This figure (Fig. 14) demonstrates how responsive the Miura origami Design is to directional load, which is important for applications and for use in its design. It exhibits significant bending behavior that is typical for folded geometry and has potential applications in deployable structures and mechanical metamaterials.

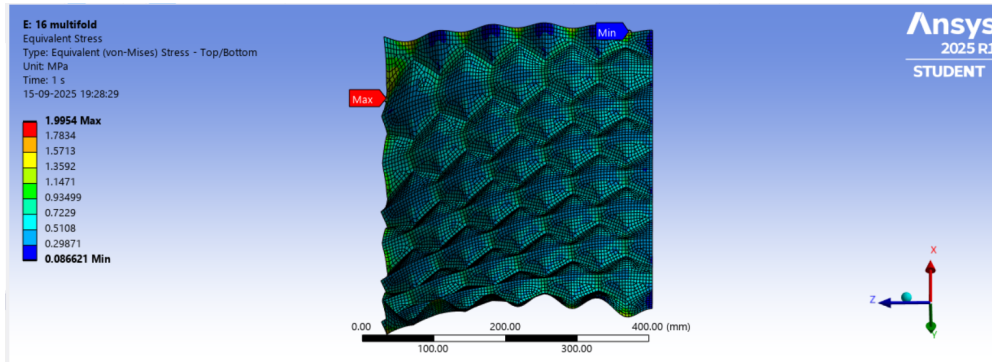


Fig 12: Equivalent stress for 15X9 miura origami

Figure 12. shows the results of an equivalent stress (Von-Mises stress) analysis for a 15x9 Miura origami structure analyzed in ANSYS 2025 R1 Student Edition. The contour plot shows the distribution of stress across the folded geometry when subject to the applied static structural load. The stress distributions are shown on the top and bottom surfaces, with the associated values provided in MPa (megapascals) units. The maximum equivalent stress is approximately 1.9954 MPa (shown in red near the top left edge), while the minimum stress is approximately 0.06621 MPa (shown in dark blue near the top right corner). The observed deformation is such that the stress distribution is non-uniform, typical of origami structures, which have complex folded geometry and load concentration at the crease junctions. The

simulation provides important insight into the material response and stress concentration locations as to the integrity and optimization of a material in the context of foldable/deployable engineering applications. The stress analysis (Fig. 15) suggests a follow up on the structural integrity or mechanical behavior under loading.

#### Miura 19X9 folds:

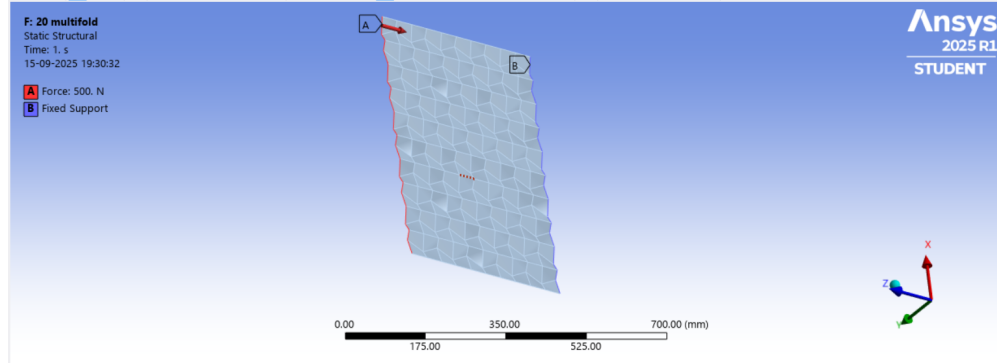


Fig 13: Force Applied and fixed support for 19X9 fold miura origami

Figure 13. depicts the boundary conditions applied for a 19x9 Miura fold origami structure in ANSYS 2025 R1 Student Edition for a static structural analysis case. The model shows a clear fixed support located in the bottom edge (point B), which restricts all degrees of freedom, thereby ensuring the edge remains fixed during simulation. The other edge (point A) is loaded with 500 N in some specified direction, most likely in the Z direction, or in some incline depending on the orientation of the geometry. This rigging structures the scope of modeling, how the Miura fold structure may behave under tension or compression, while fixed on one end. The figure (Fig. 16) is important for understanding forces of external mechanical loading interacting with the complex fold geometry, and shows structural constraints used to inform evaluations measuring deformation, stress distribution, and mechanical behavior of the origami pattern under specified and realistic mechanical loading.

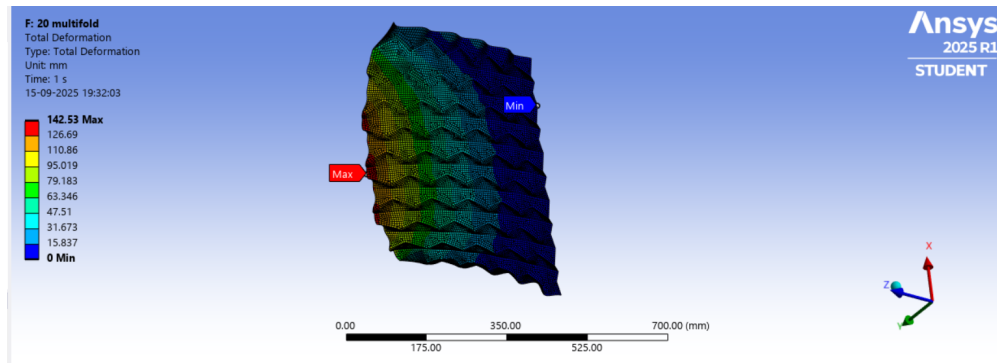


Fig 14: Total deformation for 19X9 fold origami

Figure 14. displays the total deformation results from the analysis of a 19x9 fold origami structure using ANSYS 2025 R1 Student Edition. The analysis is performed under static structural analysis, where the deformation is determined from applied loads and boundary conditions. The color contour plot illustrates the the distribution of the deformation of the structure from a minimum value (shown in blue) to a total maximum deformation of 142.63 mm (shown in red) that would occur. The results suggest that deformation is non-uniform, or varies throughout the geometry of the structure. Due to the pose of the

origami and constraints on the boundaries, the maximum deformation occurred at the left edge where the right experienced the least deformation. The plot also indicates that origami-inspired geometries can experience large displacements yet remain continuous, which can be advantageous for applications that require mobility or flexibility.

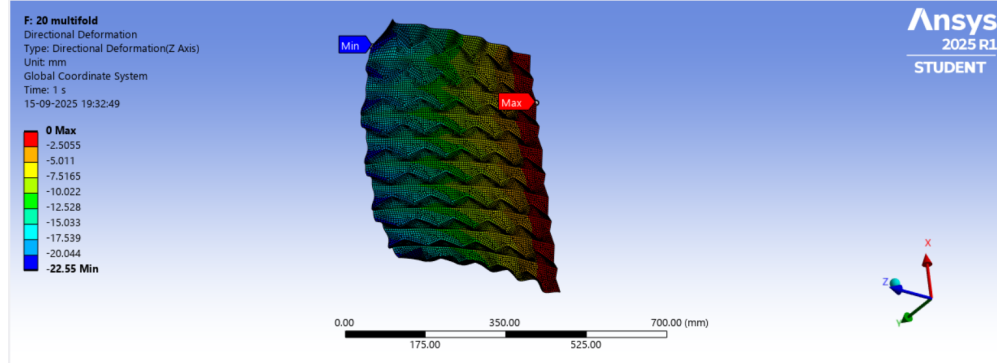


Fig 15: Directional deformation for 19X9 miura origami

Figure 15. shows the directional deformation results of a  $19 \times 9$  Miura origami structure as output by ANSYS 2025 R1 Student Edition. The analysis considers deformation in the Z-direction of the global coordinate system. The color contour map indicates the variation in deformation throughout the structure from a maximum of approximately 0 mm (red zone) to a minimum of  $-22.55$  mm (blue zone). This result shows that some areas of the origami structure have experienced downward movement while others have remained roughly stationary with a slight shift. The deformation takes place in a unique pattern that is heavily influenced by the Miura folding geometry in the origami structure, which allows the structure to respond to external loads via a unique kinematic folding action. This deformation suggests an ability to experience considerable flexibility and ability to deform in a directional way, with deployments to be used in lightweight or deployables structures.

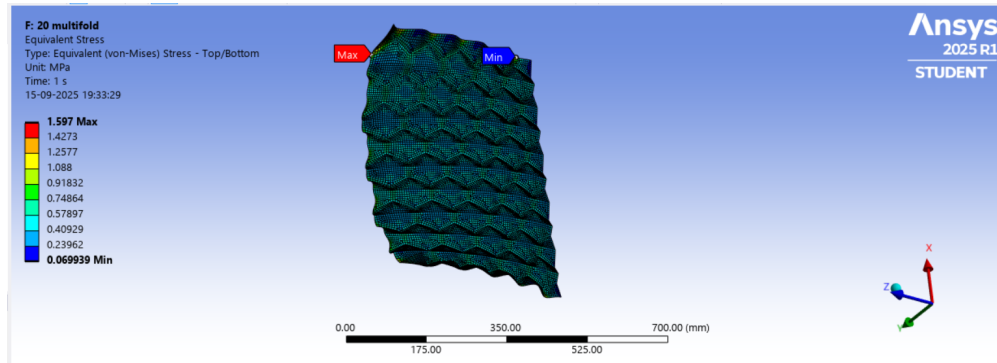


Fig 16: Equivalent stress for 19X9 miura origami

Figure 16. demonstrates the equivalent stress distribution for the Miura origami structure ( $19 \times 9$ ) analyzed in ANSYS 2025 R1, Student Edition. The analysis uses the von Mises stress criterion, which is frequently employed in assessing material yield behavior under complex loading conditions. The contour plot shows that the stresses of both types range from a minimum of  $0.069$  MPa (blue region) to a maximum of  $1.597$  MPa (red region). The higher stresses (red) are near edges of the fold where there might be localized deformation or stress concentrations due to the folding geometry, while the majority of the structure is subject to relatively low stress according to the large green and blue regions. This

stress distribution further demonstrates the utility of a Miura origami in distributing applied loads while limiting levels of stress on a majority of the structure, maintaining structural stability. These findings emphasize the promise of Miura origami in low-weight, deployable engineering applications requiring both load-bearing capability and flexibility.

### Flat plate 240x400 mm:

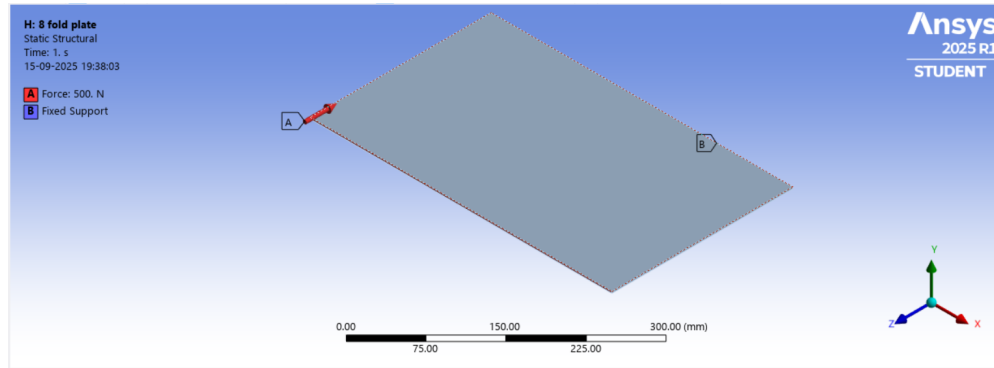


Fig 17: Force Applied and fixed support for flat plate 240x400 mm

Figure 17. depicts a finite element analysis of a flat plate, 240×400 mm in measurement, ensuring the analysis can also be seen as three-dimensional. In the main viewport, the simulation shows a rectangular plate, with boundary conditions that are applied - a fixed support (triangular symbols) at one edge, along with a force load applied downwards (red arrow). The project tree to the left is structured in a typical static structural analysis, with branches that are geometry, model, and solution. The analysis is set up as a static structural analysis, with an environmental temperature of 22°C, and can be analyzed to evaluate the stress, strain, and deformation characteristics of the plate with the given loading conditions. This is a straightforward engineering analysis that corresponds to checking structural integrity to verify if the plate can safely accommodate an operational load.

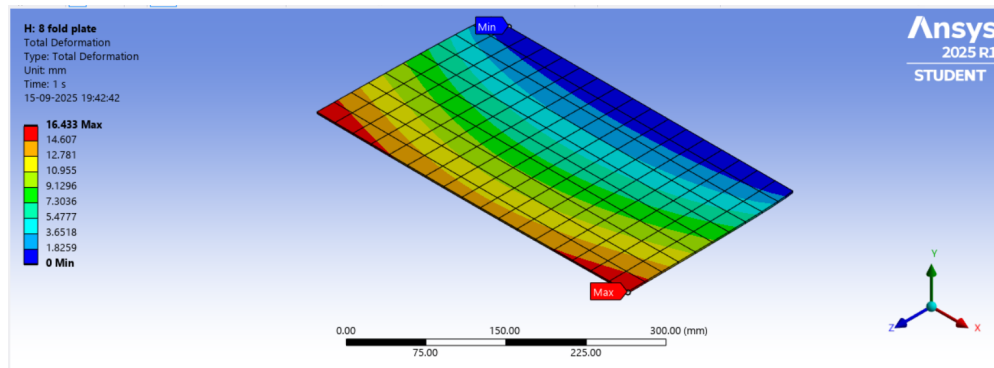


Fig 18: Total deformation for flat plate 240x400 mm

Figure 18. depicts a finite element analysis of a flat plate, measuring 240×400 mm, performed using ANSYS Mechanical. The simulation includes the display of a rectangular plate in the main viewport, boundary conditions applied to the plate - specifically, a fixed support (triangles) along one edge, and a force load (red arrow). The project tree on the left shows an example static structural analysis workflow with geometry, model, and solution branches. The analysis has been defined as a static structural

analysis, with a 22°C environment temperature and to determine the stress, strain and deformation behavior of the plate under an applied load. This is a common engineering analysis used to confirm structural integrity and verify that a plate can safely operate under applied loads.

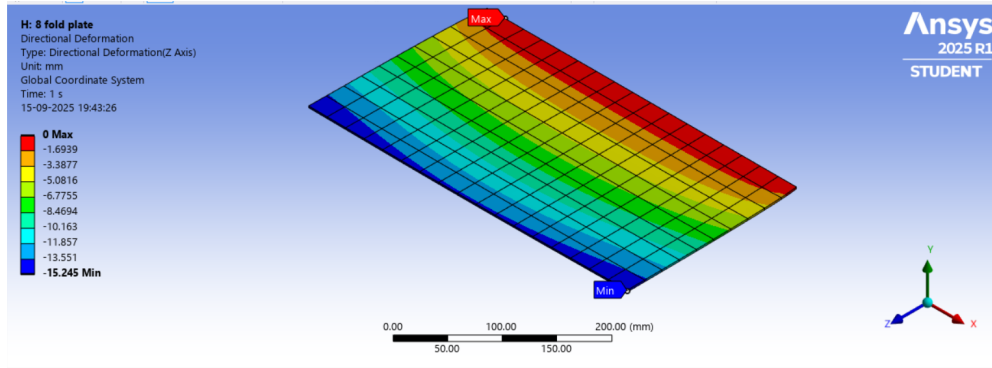


Fig 19: Directional deformation for flat plate 240x400 mm

Figure 19. displays the results of a directional deformation analysis for the 240×400 mm flat plate analyzed in ANSYS Mechanical. The contour plot demonstrates a deformation in a certain direction (probably Y-direction) with values attributed to the deformation in one direction from -15.265 mm (blue regions) to 0 mm maximum (red regions). The color scale is formatted from blue (maximum negative deformation) transitioning to green and yellow to red (zero deformation) regarding how the plate is deflecting directionally due to applied loading. The fixed support constraint indicates there is zero directional deformation (in red) and the free end reflects maximum negative directional deformation (in blue). Directional analysis like this helps engineers to understand how the structure behaves in a particular coordinate direction, which is important to understand the full behavior of the deformation and to ensure that the design is usable for the intended application with respect to directional displacement requirements.

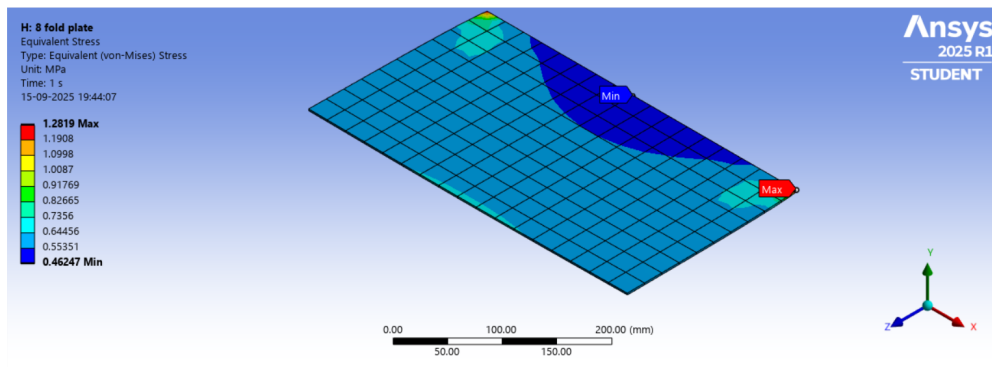


Fig 20: Equivalent stress for flat plate 240x400 mm

Figure 20. shows an ANSYS finite element analysis simulation that shows equivalent stress distribution (von Mises stress) for a flat rectangular plate measuring 240x400 mm in size. The analysis shows stress concentrated at specific locations on the plate, as represented in color-coded contour plot with indicated stress values ranging in magnitude from minimum stress of 0.44247 MPa in blue to maximum stress of 1.3519 MPa in red. The red areas are the most significant stress concentration areas that appear to be in the corner regions or constraint points of the plate, while true blue-green areas are areas of the plate that are subject to lower stress, which is around the majority of the surface area of the plate. This

analysis method is a common form of taking a structural analysis, which is frequently used in the engineering field, to highlight points of which the structure may fail. This allows the designer/engineer to know how (mechanical) loads may be allocated to the component without speculating on loading/magnitudes or where failure may occur; this understanding allows for parameters to be adjusted into in optimization. Design parameters that may be optimized into are related to geometry, thickness, material type (e.g., aluminum, 5052 aluminum), etc.

## 4. Results

Finite element simulations conducted in Ansys Workbench evaluated different origami geometries of Miura-ori across a range of structural and loading parameters. The simulation results revealed significant variation in crash performance and energy absorption:

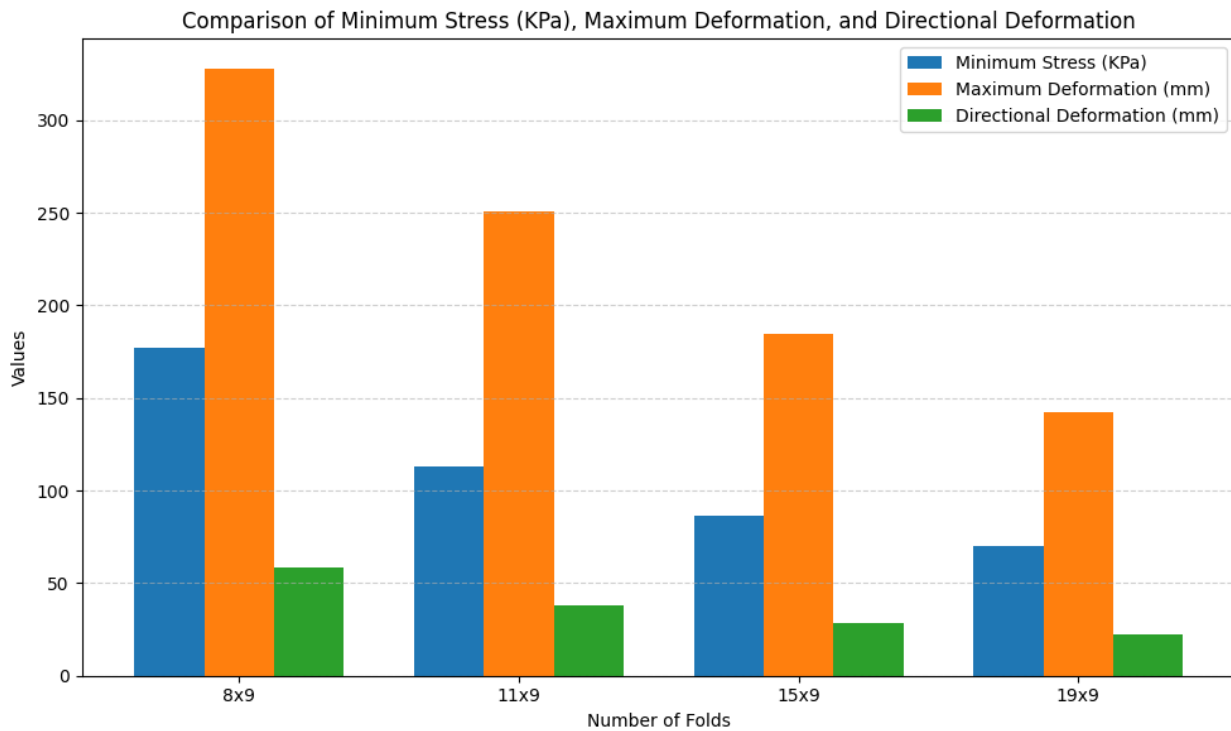


Fig 21 . miura origami

In Figure 21., the minimum stress (KPa), maximum deformation (mm), and directional deformation (mm) of four separate fold configurations of a TPU material, specifically 8x9, 11x9, 15x9, and 19x9, are displayed at a constant applied force of 500 N. It is evident from the results witnessed that with each battle configuration, all three parameters decrease with each configuration. The 8x9 configuration has the best minimum stress whilst this value declines for configurations with increasing folds. The better stress is clearly visible in the first couple of folds, supporting the idea that structures with fold configurations distribute stress better when increasing fold counts. Furthermore, the maximum deformation and directional deformation values both decrease for each increasing fold count which illustrates better of stiffness and resistance to deformation with folds. To summarize, the bar chart

provides evidence that by increasing folds will improve your structural performance due to having lower stress concentrations and less overall deformation.

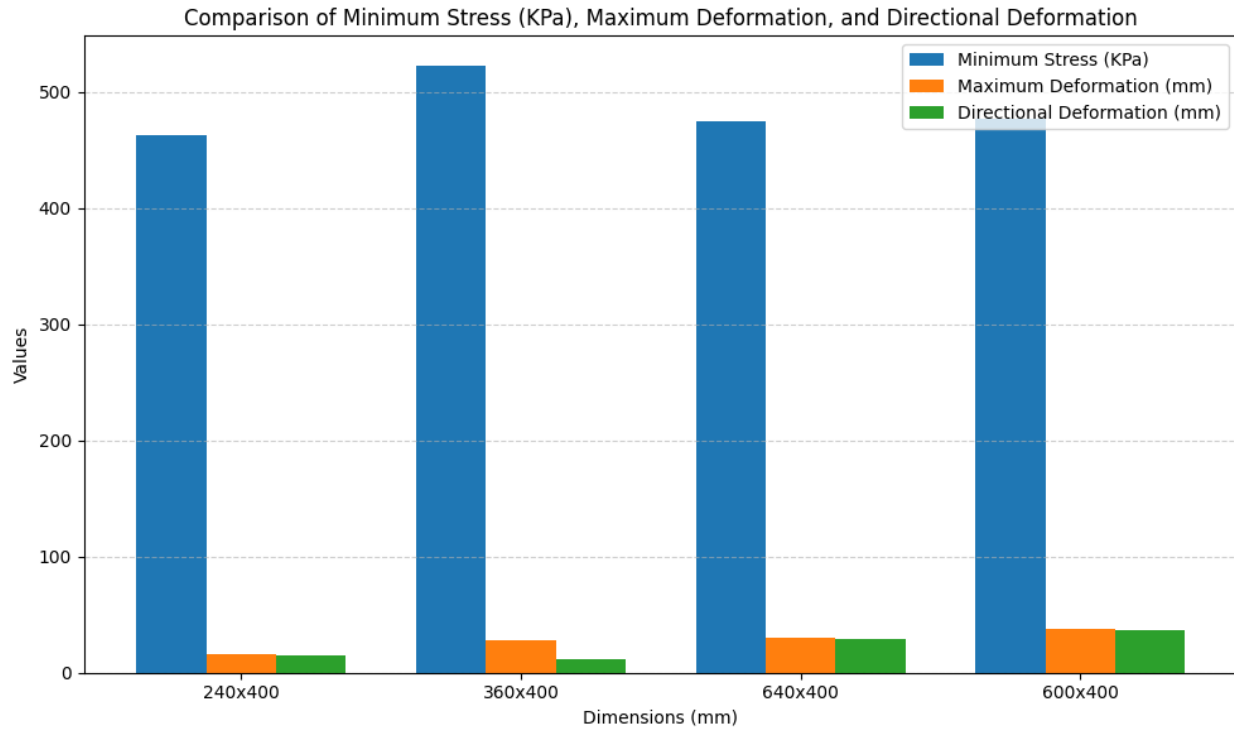


Fig 22 . flat origami

Figure 22. illustrates the structural performance of different plate sizes (240x400, 360x400, 640x400, and 600x400 mm) in terms of the three engineering parameters: minimum stress (KPa), maximum deformation (mm), and directional deformation (mm). Notably, it is interesting to observe that the 360x400 mm plate demonstrates the greatest minimum stress at approximately 520 KPa, while all the plates show comparable low (under 40 mm) maximum and directional deformation. These results demonstrate that even though stress is significantly different with respect to different plate sizes (with the 360x400 mm the most according to the results) the deformation values were consistently low with respect to all plate sizes indicating good structural stiffness for each of the tested plate sizes.

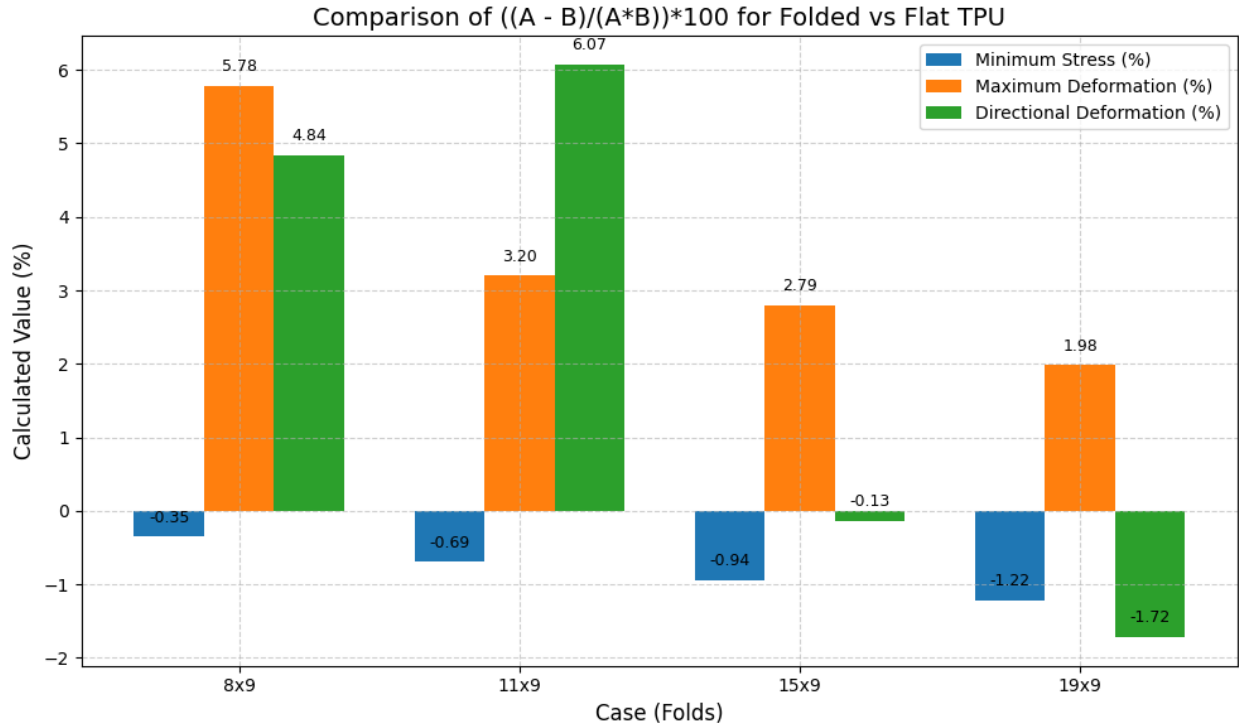


Fig 23 . folded vs flat origami

Figure 23. demonstrates the percentage difference of each of the measured minimum stress, maximum deformation, and directional deformation for Folded and Flat TPU samples in investigation of four different folding cases ( $8 \times 9$ ,  $11 \times 9$ ,  $15 \times 9$  and  $19 \times 9$ ) comparison. Folded TPU acts with a lower minimum stress (negative values) than Flat TPU exhibiting improved distribution of stress. The Folded TPU sample has increased maximum deformation and directional deformation with the first two fold cases ( $8 \times 9$  and  $11 \times 9$ ), suggesting the sample has great amounts of flexibility. However, observation of these deformation behaviors decreased for larger fold count ( $15 \times 9$  and  $19 \times 9$ ). Subsequently, the deformation values changed to either less positive or negative suggesting less deformability and an increased stiffness. In the overall view, the greatest and optimal differences were within the tests that were moderately folded ( $8 \times 9$ – $11 \times 9$ ), while the extreme folded cases had extra folding that tapered off any benefits associated with folding, while contributing to less deformation.

## 5. Conclusion

The simulation outcomes from ANSYS validate that structures having rotatable origami forms, and especially Miura-ori and functionally graded fold patterns, show excellent crashworthiness and energy absorption when subjected to axial compression. The load-bearing response capability or energy absorption characteristics can be tailored through changes in geometric parameters or to modify the structural configuration to meet a given design requirement.

The evaluations conducted under axial compression show that origami-based multifold structures deform significantly greater, and thus exhibit greater energy absorption than flat plates of the same base dimensions and constituent materials. For example, the 8-fold origami deformed on average to 89.8 mm, which is nearly 12 times greater than the 8-face flat plate that only produced 7.4 mm of deformation, with maximum deformation (peak readouts) being nearly 20 times greater. The 12-fold origami deformed, on average, to 60.6 mm, which is roughly 4.4 times greater than the deformation measured for the corresponding flat plate at 13.7 mm. The 16-fold origami deformed to 45.8 mm, which is 2.5 times greater than the deformed length measured for the flat counterpart that only produced 18.5 mm.

These results clearly demonstrate that superior compliance and energy absorption characteristics, based on the load response, have been delivered via the use of origami geometries when under axial loading. The lower density of folds (in this case, the 8-fold designs) leads to significantly greater deformation and absorption potential. When higher density folds are used (whether it be the 12 or 16-fold origami designs) the resulting imposition causes the structural assembly to stiffen, leading to lower resultant deformation over the same distance. By contrast, flat plates remain comparatively rigid, with displacements limited to under 40 mm in all cases.

## 6. References

1. Jiayao Maa, Jichao Song, Yan Chena,"An origami-inspired structure with graded stiffness" International Journal of Mechanical Sciences Volume 136, February 2018.  
[<https://doi.org/10.1016/j.ijmecsci.2017.12.026>]
2. X.M. Xiang, G. Lub, Z. You, "Energy absorption of origami inspired structures and materials" Thin-Walled Structures, Volume 157, December 2020.  
[<https://doi.org/10.1016/j.tws.2020.107130>]
3. Mojtaba Moshtaghzadeh, Pezhman Mardanpour, "Design, mechanical characteristics evaluation, and energy absorption of multi-story Kresling origami-inspired structures" Mechanics Research Communications, Volume 130, July 2023.  
[<https://doi.org/10.1016/j.mechrescom.2023.104125>]
4. Sophie Leanza et al. "Active Materials for Functional Origami" Advanced Material(2023).  
[<https://doi.org/10.1002/adma.202302066>]
5. Joseph M. Gattas, Zhong You "Miura-Base Rigid Origami: Parametrizations of Curved-Crease Geometries" Journal of Mechanical Design (2014).
6. Liu H, Plucinsky P, Feng F, James RD. 2021 Origami and materials science. Phil. Trans. R. Soc. A 379: 20200113.  
[<https://doi.org/10.1098/rsta.2020.0113>]
7. Meredith Johnson et al " Fabricating biomedical origami: a state-of-the-art review" Int J Comput Assist Radiol Surg. (2017).
8. Edwin A Peraza-Hernandez et al, "Origami-inspired active structures: a synthesis and review" Smart Materials and Structures · August 2014.
9. Larissa M. Fonseca et al "An overview of the mechanical description of origami-inspired systems and structures" International Journal of Mechanical Sciences Volume 223 (2022).

[<https://doi.org/10.1016/j.ijmecsci.2022.107316>]

10. Lisheng Mou et al “An octagonal cylindrical origami structure with variable stiffness for soft robotics”, International Journal of Mechanical Sciences, 303, (110604), (2025).  
[<https://doi.org/10.1016/j.ijmecsci.2025.110604>]
11. Chen Y, Yan J, Feng J. Geometric and Kinematic Analyses and Novel Characteristics of Origami-Inspired Structures. *Symmetry*. 2019; 11(9):1101.  
[<https://doi.org/10.3390/sym11091101>]
12. Zhou X, Zang S, You Z. 2016 “Origami mechanical metamaterials based on the Miura-derivative fold patterns”, Proc. R.Soc. A 472: 20160361.  
[<http://dx.doi.org/10.1098/rspa.2016.0361>]
13. Lu G, Yu TX. “Energy absorption of structures and materials”. First ed. Cambridge: Woodhead Publishing; 2003.
14. Song J, Chen Y, Lu G. Axial crushing of thin-walled structures with origami patterns. *Thin-Walled Structures*. 2012;54:65-71.
15. Ma J, You Z. Energy absorption of thin-walled square tubes with a prefolded origami pattern-Part I: geometry and numerical simulation. *Journal of Applied Mechanics*. 2013;81:011003.